Lab on a Chip

RSCPublishing

PAPER

View Article Online
View Journal | View Issue

Cite this: *Lab Chip*, 2013, **13**, 2937

Influence of real-world environments on the motion of catalytic bubble-propelled micromotors†

Guanjia Zhao, Hong Wang, Bahareh Khezri, Richard D. Webster and Martin Pumera*

Received 10th April 2013,
Accepted 13th May 2013

DOI: 10.1039/c3lc50446h

www.rsc.org/loc

Self-propelled autonomous micromachines have recently been tasked to carry out various roles in real environments. In this study, we expose the microjets to various types of water that are present in the real world, examples include tap water, rain water, lake water and sea water, and we sought to investigate their behaviors under real world conditions. We observed that the viability and mobility of the catalytic bubble jet engines are strongly influenced by the type of environmental water sample. Amongst the four water samples tested, the seawater sample exhibits the strongest influence, completely disabling any motions arising from the microjets. The motion of the microjets is also reduced in tap water, which contains large quantities of inorganic ions that have been purposely introduced into tap water *via* processing in water treatment plants. Lake water and rain water samples exhibited the least influence on the microjet's motion. All of the four water samples were also characterized by determining their ion compositions and conductivities, and we will show that there is a distinct correlation between the reduced mobility of the microjets with the ion content of the water found in real environments.

Introduction

Self-propelled nano and micromachines are presently at the forefront of nanotechnology research.[1–6] These micromachines have been carefully designed to perform various applied tasks, such as performing microsurgeries,[7] guided drug delivery,[8] natural resources discovery[9] or environmental remediation.[10] The mobility of these nano and micromachines proceed *via* propulsion mechanisms, which range from diffusiophoresis[11] and self-electrophoresis[12] to bubble-jet ejection.[6] Although diffusiophoresis and self-electrophoresis are involved in the mechanism, the propulsion force provided by them is relatively low when compared to the bubble-ejection mechanism. At the moment, the catalytic bubble-propelling micromachines have proven to be highly popular due to their high power output.[13]

There has been much discussion on the utilization of these catalytic microjet motors to perform useful tasks in applications, such as biomedicine, environmental clean-up or the discovery of natural resources.[7–10] However, most of the experimental set-ups in reported papers use distilled water as the medium for the motion of microjets and we consider such medium to be unrealistic, especially if these microjets have uses in real-world applications. It has been demonstrated recently that compounds, such as extracellular thiols or organic solvents, can significantly hamper the propulsion of these catalytic microjets due to poisoning of the Pt catalyst, or the quenching of the disproportionation reaction of fuel molecules.[14] It was also found that the blood components exhibited major problems for the motion of microjet engines.[15]

Here, we wish to investigate how real-world environments can influence the motions of microjets. We will show that the mobility of catalytic microjets can be strongly influenced depending on whether they move in tap water, lake water, rain water or seawater, when compared to their motion in distilled water. These findings shall have a profound impact on how we envision the applications of these micromachines.

Experimental section

Materials

The cyclopore polycarbonate membranes with pores of 2 μm in diameter were purchased from Whatman, USA (Cat. No.: 7060-2511). The pores are conical in shape. Colloidal graphite (isopropanol base) was purchased from Ted Pella, Inc. (Lot No.: 12009-2, USA). Hydrogen peroxide (27%, Lot No.: 10151507) was purchased from Alfa Aesar, Singapore. Methylene chloride and ethanol were purchased from Tedia, USA. $CuSO_4 \cdot 5H_2O$ (98+ %) and sodium dodecylsulfate (SDS, Lot No.: 079K0335) were purchased from Sigma-Aldrich. The

---

Division of Chemistry & Biological Chemistry, School of Physical and Mathematical Sciences, Nanyang Technological University, Singapore 637371, Singapore. E-mail: pumera@ntu.edu.sg

† Electronic supplementary information (ESI) available: SEM image of microjet, mobility of microjets in KNO_3 solution and motion pictures. See DOI: 10.1039/c3lc50446h

platinum plating solution (Lot No. 20251001) was obtained from Technic Inc., USA. The chemicals were used as received and ultrapure water (18.2 MΩ cm) from a Millipore Milli-Q purification system was used throughout the experiments. Water samples were all collected in Singapore. Sea water sample was collected from the East Coast of Singapore, lake water was from the Nanyang Lake in Nanyang Technological University (NTU) campus, Singapore, rain water was collected on a building roof of 30 meters high in the western area of Singapore, and tap water was from the laboratory tap water in Nanyang Technological University, Singapore.

Apparatus

Electrochemical deposition was carried out with a μAutolab type III electrochemical analyzer (Eco Chemie, the Netherlands) connected to a computer and controlled by General Purpose Electrochemical Systems version 4.9 software (Eco Chemie). The deposition procedure was conducted at room temperature (23 °C) using a three-electrode arrangement. A platinum electrode was utilized as a counter electrode, and Ag/AgCl was used as a reference electrode (CH Instruments, Inc., USA). The ultrasonication process was carried out with a Fisherbrand FB 11203 ultrasonicator, and centrifugation was carried out with a Beckman Coulter Allegra 64R centrifuge. Scanning electron microscopy (SEM/EDX) analysis was obtained with a JEOL JSM 7600F instrument.

Methods

Synthesis and characterizations of Cu/Pt concentric bimetallic microtubes. The Cu/Pt concentric bimetallic microtubes were synthesized with a modified electrochemical deposition procedure on a cyclopore polycarbonate template.[16] Colloidal graphite ink was applied on one side of the polycarbonate template with commercial cotton swabs. A piece of flattened aluminium foil was attached to the ink immediately, which serves as a working electrode for the plating experiments. The template was assembled into a customized electrochemical deposition cell. The template was rinsed with 5 mL of ultrapure water (18.2 MΩ cm) 4 times, and the Cu outer layer was deposited galvanostatically at −4 mA for 450 s in a deposition solution which contained 1 M $CuSO_4$. Consequently, after removing the deposition solution, the template was rinsed 5 times with 8 mL of water. The platinum segment was subsequently electrodeposited at −4 mA for 450 s each, using a commercial plating solution. When the deposition of the Pt layer on the microtubes was completed, the electrochemical cell was disassembled and the template was washed 5 times with 8 mL of water each. After that, the template was ultrasonicated 3 times in 2 mL of water for 3 min each time. The graphite layer was removed during the ultrasonication procedure. The template was placed in an Eppendorf tube with 2 mL of methylene chloride and ultrasonicated until the whole template was dissolved. The electrochemically deposited microtubes were collected as a pellet from a centrifugation step at 6000 rpm for 3 min and subsequently washed repeatedly 3 times with methylene chloride. The solution was then washed with ethanol and water 2 times each and centrifuged for 3 min after each washing step. The microtubes were stored in water at room temperature. Scanning electron micrographs for microjets are shown in Fig. S1 ESI†.

Operation of microjets. The microjets were set into motion for propulsions in aqueous solutions containing various concentrations of water samples, a fixed concentration of hydrogen peroxide (3%) and a fixed surfactant concentration (SDS, 1 wt%). A mixture of microjets (5 μL), SDS (1 wt%), H_2O_2 (3 wt%) together with the tested water samples were applied on a glass slide freshly cleaned with nitrogen gas. The behaviors of the microjets were then observed under a microscope. Optical microscope videos and images were obtained with Nikon Eclipse 50i microscope. Video sequences were processed with Nikon NIS-Elements™ software.

Ion Chromatography (IC). Cation IC experiments were performed with a Dionex ISC-900 utilizing an Ion Pac CS12A 4 mm × 250 mm analytical column. For cation IC, the eluent consisted of 20 mM methanesulfonic acid, and the chemical regenerant consisted of 100 mM tetrabutylammonium hydroxide. Anion IC experiments were performed with a Dionex ICS-1100 utilizing an Ion Pac AS22 4 mm × 250 mm analytical column. For anion IC, the eluent consisted of 4.5 mM sodium carbonate and 1.4 mM sodium bicarbonate, and an electrochemical suppressor was used.

Conductivity measurements. These were performed with a Radiometer IONcheck 30 probe.

Results and discussion

We have studied the motions of Cu/Pt catalytic microjets, which were prepared by the template-directed electrodeposition, as described in the Experimental section.[16] These microjets exhibit a conical shape, with a length of 7 μm, and the diameters at opposite ends are 1.5 and 2 μm. The propulsion of the microjet is driven by the catalytic decomposition of hydrogen peroxide at its inner surface, creating bubbles, which are expelled at the end of the microjet, thereby propelling it forward.[17]

We wish to investigate the extent to which real-world environments can influence the motion of microjets. We investigated common water environments, such as tap water and environmental waters, such as rain water, lake water and seawater. The distilled water was used as the control environment to which the motion of the microjets can be compared with. In particular, we decided to focus on the ratio of the microjets expelling bubbles in the given environment, as well as on the ratio of microjets moving in the given media. In addition, for the jets which exhibited motion, their average velocities were also determined. In all of the experiments, the concentration of fuel (H_2O_2) used is 3 wt% in all cases.

We first evaluated the motion of the microjets in tap water. As shown in Fig. 1A, while 100% of the microjets ejected bubbles and showed mobility in distilled water; only 19% of microjets ejected bubbles in tap water and only 15% exhibited motion. The average velocity of the microjet engines in distilled water is 365 μm s^{-1}, while the velocity of the microjets in a maximum concentration (71.5%) of tap water

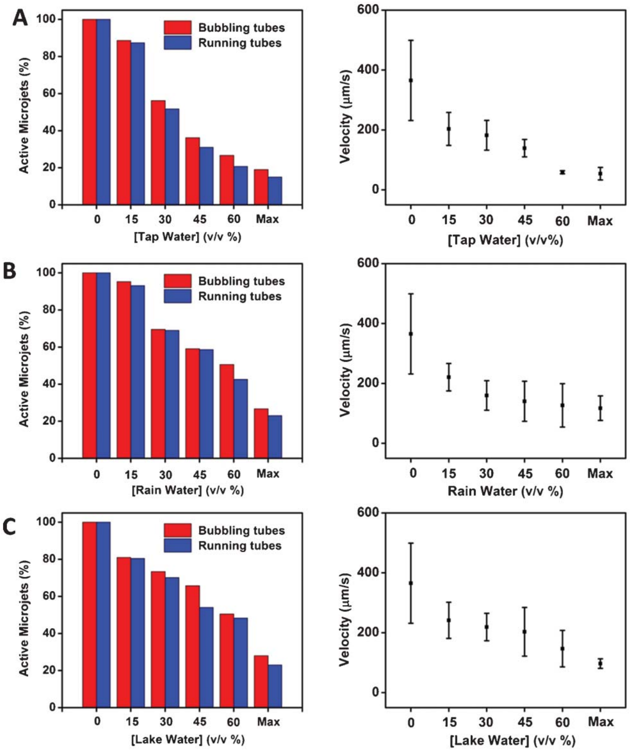

Fig. 1 Motion of the catalytic microjets (prepared by electrochemical template deposition method) in various real-world waters. (A) tap water, (B) rain water and (C) lake water. Left: Graph showing the influence of the natural water concentration (as diluted with distilled water) on the activity of the microjets, which exhibited either bubble ejection (red bar) or microjet motion (blue bar). Right: Graph showing the influence of the concentration of natural waters on the velocity of the moving microjet engines. Conditions in the all experiments: temperature of 23 °C, 3% (wt.) H_2O_2 and 1 (wt.)% SDS.

is merely 54 μm s^{-1}. Note that the fuel used is 3% H_2O_2 in tap water prepared from a 27% (wt.) stock solution and later added to the tap water, therefore the maximum concentration of tap water was 71.5% (indicated in the Figures as ''Max''). In order to investigate whether the decrease in the mobility of the microjets takes places gradually or in a single step, we prepared mixtures of tap water with distilled water at different concentrations (v/v). We found that the decrease in mobility of the microjets was gradual over the concentration range, as shown in Fig. 1A. For motion pictures of the movement of microjets in distilled water and ''Max'' concentration of tap water, see Video S1 and S2, ESI†, respectively.

Next, we turned our attention to the rain water sample. Similar to the previous example, the viability of the microjets in rain water (with 3% H_2O_2) was much lower than that in distilled water, with only 27% of the microjets ejecting bubbles and 23% of the microjets exhibiting motion. The average velocity of the mobile microjets in rain water was 117 μm s^{-1}, which is significantly lower than that in the distilled water (365 μm s^{-1}). As in the case of tap water, when rain water was mixed with distilled water, the viability and mobility decreased gradually with a corresponding increase in the fraction of rain water present (Fig. 1B). For a motion picture of the movement of a microjet in ''Max'' concentration of rain water, see Video S3, ESI†. The exact levels of organic compounds in the water samples are currently not available. Nevertheless, the tap water is purified to high standards with organic compounds having values in the very low ppm to ppt levels. A recent study on atmospheric gaseous compounds identified 48 volatile organic compounds in Singapore,[18] but these are not likely to enter the water to a significant amount (compared to the concentrations of inorganic ions).

Subsequently, we investigated the motion of the microjets in natural fresh water reservoir. The mobility of the microjets in lake water is lower when compared with distilled water; only 28% of the microjets ejected bubbles and 23% were observed to show motion (Fig. 1C). The velocity of the microjets in lake water is 97 μm s^{-1}. Interestingly, the mobility of the microjets in lake water is somewhat similar to that of the rain water sample. The mobility of microjets was also shown to gradually decrease upon increasing the fraction of lake water in distilled water (Fig. 1C). For a motion picture of the movement of a microjet in ''Max'' concentration of fresh lake water, see Video S4, ESI†. It should be noted that mobility of the microjets is higher in rain or lake water than in tap water. We will discuss the reasons in the following text. Relative standard deviations (RSD) for velocity data points in Fig. 1A are 36.6%, 27.7%, 27.7%, 21% and 8.7% for 0, 15, 30, 45 and 60% (v/v) of tap water, respectively. RSD for data presented in Fig. 1B are 36.6%, 20.8%, 31%, 48% 57% for 0, 15, 30, 45 and 60% (v/v) rain water, respectively. RSD for data presented in Fig. 1C are 36.6%, 25%, 21%, 40%, 41.4% for 0, 15, 30, 45 and 60% (v/v) lake water, respectively.

Lastly, we investigated the mobility of microjets in the seawater sample. It was previously suggested that bubble-propelling microjets are capable of performing environmental clean-up of oil spills,[10a] which strongly implies that such operation takes place in seawater. However, when we immersed the microjets in seawater (containing 3% wt of H_2O_2), we observed no motion. When we examined the influence of seawater content in seawater/distilled water mixture, we observed a dramatic decrease of the mobility of microjets, at 6% (v/v) seawater whereby only 47% of microjets ejected bubbles and no more than 41% move with an average velocity of 63 μm s^{-1} (compared to 365 μm s^{-1} in distilled water), see Fig. 2A. For a motion picture of the movement of a microjet in 6% sea water, see Video S5, ESI†. At 9% (v/v) of seawater, only 8.6% of the catalytic microengines ejected bubbles, and 1% exhibited motion. The striking differences between the motions of the microjets in the fresh-water sources and in seawater led us to the hypothesis that the motion of the microjets is influenced by the amount of inorganic ions present in the environment. To test this hypothesis, we first performed the experiment in a NaCl solution. As seawater contains NaCl at a large concentration of approximately 35 g L^{-1}, NaCl itself is sometimes used to simulate an ''artificial seawater'' environment (Fig. 2B); hence we studied whether the microjets move in a 35 g L^{-1} NaCl solution. We did not observe any bubble ejection or motion of

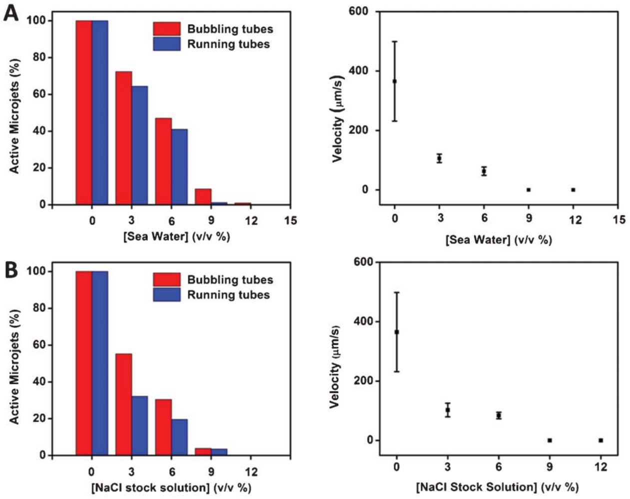

Fig. 2 Motion of the catalytic microjets (prepared by electrochemical template deposition method) in various fractions of (A) seawater, (B) 35 g L^{-1} NaCl stock solution. Left: A graph showing the influence of the seawater or NaCl stock solution concentration (as diluted with distilled water) on the activity of the microjets, which exhibited either bubble ejection (red bar) or microjet motion (blue bar). Right: A graph showing the influence of the concentration of seawater or NaCl stock solution on the velocity of the moving microjet engines. Conditions in all of the experiments: temperature 23 °C, 3% (wt.) H_2O_2 and 1 (wt.)% SDS.

microjets, leading us to study how diluted NaCl solutions can influence the motions of the microjets. We observed a very similar decrease in the viability of the microjets in diluted seawater, with bubble ejection being reduced to 30% in 6% of NaCl solution (35 g L^{-1} NaCl being considered as 100%) and only 20% of microjets were moving, with a reduced speed of 84 μm s^{-1} (Fig. 2B). At 9% NaCl solution, only 3.8% of microjets produced bubbles and 3.4% move at a velocity that is nearly 0 μm s^{-1}; and at 12% NaCl, no motion of microjets was observed. Therefore we have demonstrated that in contrary to previous observations,[19] the motion of the Pt catalytic bubble microjet is highly influenced by the salt concentration in the environment, which is similar to the motion of self-electrophoretically propelled microrods.[12,20] It should be noted that a similar experiment with rolled-up microjets (dimensions 50 × 5 μm) was also performed,[21] and no motion was observed in seawater at 3% H_2O_2 either. Note that the decreased mobility of microjets is not caused only by the NaCl solution, but by solution of other salts as well. Fig. S2 (ESI†) shows a similar trend for KNO_3 solution.

To explore this issue in a greater detail, and in order to explain the differences in the decrease of the mobility of microjets in fresh water sources, we determined the inorganic ion compositions of the water samples using ion chromatography and conductivity measurements.[22] It can be observed from Table 1 that tap water contains the largest amounts of inorganic ions, such as F^-, Cl^-, SO_4^-, Na^+, K^+, Ca^{2+}, Mg^{2+} *etc.*, much more than in lake water or rain water. This is also reflected in the higher conductivity reading of 137 μS cm^{-1} for tap water, as compared to the rain and lake water conductivities of 33 and 41 μS cm^{-1}, respectively. The amount of ionic components of the solution directly correlates to the decreased viability and mobility of microjets.

Table 1 Mean concentration of ions is in mg L^{-1} (equivalent to ppm) of the common chemical compositions in water samples measured by ion chromatography

[Ion] (mg L^{-1})	Tap water	Rain water	Lake water
F^-	0.46	0.05	0.028
Cl^-	14.39	1.44	3.80
NO_3^-	2.02	1.48	0
SO_4^-	19.49	3.08	2.36
Na^+	6.99	0.47	2.49
NH_4^+	0.51	0.28	0.44
K^+	3.67	0.37	0.58
Mg^{2+}	0.96	0.080	0.47
Ca^{2+}	13.89	0.73	6.32

Conclusions

In our investigations, we carefully examined the behavior of the microjets in various real-world water samples, as opposed to only testing them in distilled water. The real-world samples include tap water, rain water, lake water, and sea water and it was found that the samples have an influence on the motion of the microjets. In all cases for the different water samples, the motion of the Pt-catalyzed bubble-propelling microjets was discovered to be crippled to some extent, and such partial paralyzation of the motion of microjets corresponds directly to the inorganic ion composition in the natural waters. Therefore, our present study has a profound implication on the practical applications of the microjets in real-world environments.

Acknowledgements

M.P. thanks NAP and JSPS-NTU for partial financial support.

References

1 W. F. Paxton, S. Sundararajan, T. E. Mallouk and A. Sen, Chemical Locomotion, *Angew. Chem., Int. Ed.*, 2006, **45**, 5420–5429.
2 S. Sanchez and M. Pumera, Nanorobots: The Ultimate Wireless Self-Propelled Sensing and Actuating Devices, *Chem.–Asian J.*, 2009, **4**, 1402–1410.
3 P. Fisher and A. Ghosh, Magnetically Actuated Propulsion at Low Reynolds Numbers: towards Nanoscale Control, *Nanoscale*, 2011, **3**, 557–563.
4 S. Sengupta, M. Ibele and A. Sen, Fantastic Voyage: Designing Self-Powered Nanorobots, *Angew. Chem., Int. Ed.*, 2012, **51**, 8434–8445.
5 J. Wang, Can Man-Made Nanomachines Compete with Nature Biomotors?, *ACS Nano*, 2009, **3**, 4–9.

6 Y. F. Mei, A. A. Solovev, S. Sanchez and O. G. Schmidt, Rolled-up Nanotech on Polymers: from Basic Perception to Self-Propelled Catalytic Microengines, *Chem. Soc. Rev.*, 2011, **40**, 2109–2119.

7 X. Wang, A. A. Solovev, A. N. Ananth, D. H. Gracias, S. Sanchez and O. G. Schmidt, Rolled-up Magnetic Microdrillers: towards Remotely Controlled Minimally Invasive Surgery, *Nanoscale*, 2013, **5**, 1294–1297.

8 D. Patra, S. Sengupta, W. Duan, H. Zhang, R. Pavlick and A. Sen, Intelligent, self-powered, drug delivery systems, *Nanoscale*, 2013, **5**, 1273–1283.

9 A. Sen, M. Ibele, Y. Honga and D. Velegol, Chemo and Phototactic Nano/microbots, *Faraday Discuss.*, 2009, **143**, 15–27.

10 (*a*) M. Guix, J. Orozco, M. Garcıa, W. Gao, S. Sattayasamitsathit, A. Merkoçi, A. Escarpa and J. Wang, Superhydrophobic Alkanethiol-Coated Microsubmarines for Effective Removal of Oil, *ACS Nano*, 2012, **6**, 4445–4451; (*b*) G. Zhao, T. H. Seah and M. Pumera, External-Energy-Independent Polymer Capsule Motors and Their Cooperative Behaviors, *Chem.–Eur. J.*, 2011, **17**, 12020–12026.

11 M. Ibele, T. E. Mallouk and A. Sen, Schooling Behavior of Light-Powered Autonomous Micromotors in Water, *Angew. Chem., Int. Ed.*, 2009, **48**, 3308–3312.

12 M. Pumera, Electrochemically Powered Self-Propelled Electrophoretic Nanosubmarines, *Nanoscale*, 2010, **2**, 1643–1649.

13 W. Gao, S. Sattayasamitsathit and J. Wang, Catalytically propelled micro-/nanomotors: how fast can they move?, *Chem. Rec.*, 2012, **12**, 224–231.

14 G. Zhao, S. Sanchez, O. G. Schmidt and M. Pumera, Poisoning of bubble propelled catalytic micromotors: the chemical environment matters, *Nanoscale*, 2013, **5**, 2909–2914.

15 G. Zhao, M. Viehrig and M. Pumera, Challenges of the Movement of Catalytic Micromotors in Blood, *Lab Chip*, 2013, **13**, 1930–1936.

16 G. Zhao and M. Pumera, Concentric bimetallic microjets by electrodeposition, *RSC Adv.*, 2013, **3**, 3963–3966.

17 Y. F. Mei, G. Huang, A. A. Solovev, E. Bermudez Urena, I. Monch, F. Ding, T. Reindl, R. K. Y. Fu, P. K. Chu and O. G. Schmidt, Versatile Approach for Integrative and Functionalized Tubes by Strain Engineering of Nanomembranes on Polymers, *Adv. Mater.*, 2008, **20**, 4085–4090.

18 G. K. S. Wong, S. J. Ng and R. D. Webster, Quantitative Analysis of Volatile Organic Pollutants in Ambient Air by Thermal Desorption Gas Chromatography Mass Spectrometry, *Anal. Methods*, 2013, **5**, 219–230.

19 K. M. Manesh, M. Cardona, R. Yuan, M. Clark, D. Kagan, S. Balasubramanian and J. Wang, Template-Assisted Fabrication of Salt-Independent Catalytic Tubular Microengines, *ACS Nano*, 2010, **4**, 1799–1804.

20 W. F. Paxton, A. Sen and T. E. Mallouk, Motility of Catalytic Nanoparticles through Self-Generated Forces, *Chem.–Eur. J.*, 2005, **11**, 6462–6470.

21 A. A. Solovev, S. Sanchez, M. Pumera, Y. F. Mei and O. G. Schmidt, Magnetic Control of Tubular Catalytic Microbots for the Transport, Assembly, and Delivery of Micro-objects, *Adv. Funct. Mater.*, 2010, **20**, 2430–2435.

22 B. Khezri, Chemical analysis and statistical study on the composition of airborne particulate matter (PM2.5 and PM10), aerosols (PM2.5) inorganic trace gases and precipitation in Singapore Between 2009–2012. *Thesis*, 2013.